bioresources.com

Suitability of Thin- Layer Drying Models for Halogen Lamp Drying of Sugarcane Bagasse

Mohammad Arabi * and Mohammad Dahmardeh Ghalehno

The drying process of bagasse particles was investigated in this study using an artificial neural network (ANN) and 18 thin-layer drying (TLD) models. These models are used for investigating kinetics and understanding engineering parameters involved in the drying process of food and agricultural products. Bagasse particles were studied at 105 to 135 °C and an initial moisture content of 180% (based on the dry weight) using a halogen moisture analyzer. The results showed that an increase in the temperature decreased the bagasse drying period and increased the constant drying. The whole drying process of bagasse happened in a falling drying rate period. The fitness of drying curves on semi-experimental TLD models based on statistical parameters, including root mean square error (RMSE), sum of square errors (SSE), and coefficient of determination (R^2) showed that the Hii *et al.* model had the highest coefficient of determination and the lowest error percentage. The ANN predicted changes in the bagasse moisture content through time more accurately than the Hii *et al* model. Also, the results demonstrated that the selected ANN model and a number of semi-empirical models with less than 3 adjustable parameters provided good agreement and can be considered promising tools to predict drying kinetic of bagasse particles.

INTRODUCTION

Bagasse is essentially the fiber-based residue of the sugarcane's stalk after the process of syrup extraction. Bagasse is a renewable, sustainable, eco-friendly, bio-degradable, and cheap raw material that is used very frequently on the industrial scale. For instance, bagasse is used as a fiber and as biofuel in the papermaking industries, and it is used to manufacture sugar, bio-alcohol, yeast, animal feed, and wood composites such as MDF and particleboard (Martinez-He rnandez *et al*. 2018). In Iran, sugarcane can only be cultivated and exploited in Khuzestan province. Historical evidence indicates that sugarcane cultivation in this province dates back to 2000 years ago. The name of this province means the sugar region, which denotes the great importance of sugarcane cultivation and sugar production to the economy of this region in the past. Iranian sugarcane production facilities annually produce nearly 1.2 million tons of excess bagasse, which is burned due to the lack of conversion industries. Burning and eliminating bagasse cause greenhouse gas emission, which contributes to climate change. Burning agricultural residues directly in the field is largely responsible for the production of CO_2 (40%), CO (32%), and dust (20%) in the earth's atmosphere (Kambis and Leivne 1996; Ravindra *et al*.

2019). In addition to emitting pollutant gases and causing drastic environmental impacts, burning damp agricultural residue impoverishes agricultural fields as it depletes carbon molecules (which should be stored in the soil) by sending them back to the atmosphere (Lemieux *et al*. 2004; Zhang *et al*. 2011; Adejumo and Adebiyi 2020). Additionally, burning bagasse is a threat to human health, as a higher occurrence of asthma attack is correlated with the burning time of bagasse (Boopathy *et al*. 2002).

Fortunately, bagasse can be used as a lignocellulosic feedstock in various industries, which avoids the overexploitation of other nonrenewable lignocellulosic sources. The industrialized use of bagasse is negatively impacted by high moisture content; the processed bagasse contains 50% moisture (based on wet weight). Moisture compromises the industrialized use of bagasse and reduces both the bagasse burning rate and energy production efficiency, which are the main obstacles to the application of wet bagasse as the energy supplier in sugarcane manufacturing (Bahadori *et al*. 2012). A 3 to 4% decrease in the bagasse moisture content increases the gross calorific value and boiler efficiency by 700 to 800 KJ/kg and 1.5 to 2%, respectively (Sudhakaran and Vijay 2013). This is because the moisture content of bagasse particles must be reduced to 8% before they are used in the production of wood composites such as particleboard and MDF (Pang 2000). A high level of moisture in the bagasse passing through the dryer increases the vapor pressure in the board thickness and bowing of the board after the pressing process. Therefore, it is essential to control the final moisture of processed raw materials from the dryer, but this is time-consuming and problematic in traditional methods such as using an oven. The use of halogen dryers is a rapid method for determining the percentage of moisture in the production lines of different industries and controlling the final moisture content of processed materials (Raj and Stalin 2016; Sicoe *et al*. 2018).

Although hot air dryers are most commonly used for drying agricultural residue and lignocellulosic materials, their efficiency in the falling rate period of drying is lower than radiant dryers such as halogen lamps. This is because the temperature is directly (without any contact with the surrounding air) brought to the surface of materials under drying, resulting in an increase in the rate of heat transfer to the surface of solid materials (Sharma and Prasad 2001; Al-Hilphy *et al*. 2021; Huang *et al*. 2021). Du *et al* (2005) and Huang *et al.* (2021) studied the drying process of wood strands and lignocellulosic biomass by microwave heating dryers and concluded that these dryers functioned more effectively than hot air dryers at moisture contents below the fiber saturation point (FSP) point.

Drying of materials is a complicated process because mass and temperature are simultaneously transferred inside the material and its surrounding environment (Midilli *et al.* 2002; Erbay and Icier 2009; Ghazanfari *et al.* 2016; Ertekin and Firat 2017). Drying lignocellulosic biomass is also a complex, dynamic, highly nonlinear, and energy-intensive process involving simultaneous heat and mass transfer (Ribeiro *et al.* 2019; Han *et al*. 2020; EL-Mesery *et al*. 2022). The theoretical modeling of lignocellulosic biomass drying is very complicated because lignocellulosic biomass fiber shrinks anisotropically during the drying process (Sander *et al*. 2001; Soni 2007). It seems that semi-empirical thin-layer drying models developed on a laboratory scale are a suitable option for examining the drying kinetics of biomass materials (Babalis *et al*. 2006; Demir *et al*. 2007; Doymaz 2007a; Hii *et al*. 2009). Thin-layer drying (TLD) models and curves, which are known as specific curves of the drying rate, have been used to characterize agricultural residues and their drying kinetics (Verma *et al*. 1985; Kaleta and Górnicki 2010; Gan and Poh 2014;; Buzrul 2022).

The models and curves of TLD and convective dryers have been used to study the drying kinetics of food materials (Wang and Singh 1978; Vega *et al*. 2007; Kumar *et al*. 2012), agricultural products (Lee and Kim 2009; Kaleta *et al*. 2013; Kaur and Singh 2014), lignocellulosic biomass (Zarea Hosseinabadi *et al*. 2012; Arabi *et al*. 2017; Brys *et al*. 2021), and sugarcane bagasse (Freire *et al*. 2001; Vijayaraj and Saravanan 2007; Shah and Joshi 2010). However, the effect of halogen rays has not yet been studied on bagasse particle drying kinetics. Halogen dryers represent an innovative, fast, and very accurate method for determining the moisture content in a wide range of materials (Kambis and Leivne 1996; Ravindra *et al*. 2019). For example, the ASTM D6980 (2012) standard describes a standard test for determining moisture content and drying plastic granules using a halogen moisture analyzer. This is the first study to investigate the sugarcane bagasse drying process with halogen lamps. The drying process of agricultural and lignocellulosic materials usually takes place in three different periods, including constant drying rate, the first falling rate period of drying, and the second falling rate period of drying (Ghazanfari *et al*. 2006). Low energy efficiency and lengthy drying periods are important disadvantages of hot-air drying. In hot-air dryers, the heat transfer to the inner parts of materials under drying is limited, and energy efficiency is low owing to low thermal conductivity, leading to longer periods to dry materials (Du *et al.* 2005; Huang *et al*. 2016). In this study, the bagasse particles' drying process with halogen rays was investigated to solve the mentioned problem, avoid low thermal conductivity and energy inefficiency, and obtain an effective thermal process. In addition to TLD models, the neural network (NN) is one of the latest modeling techniques and predicts complicated physical processes that can predict materials' drying kinetics very accurately. The NN has been used for modeling the drying kinetics of agricultural products and the drying process of wood (Celma *et al*. 2008; Dash *et al*. 2020; Saxena *et al*. 2022). The results of previous studies clearly show that the ANN predicts the drying process of materials more effectively than TLD models (Chai *et al*. 2019; Sadeghi *et al*. 2019).

Therefore, the objectives of this study were to study bagasse drying kinetics and the effect of temperature on the process of bagasse drying using a halogen lamp dryer; to fit bagasse drying curves on TLD models; to determine the most appropriate model; and to predict the bagasse moisture content over time using an artificial neural network (ANN).

EXPERIMENTAL

Materials

Bagasse particles used in this study were obtained from the Neopan Karon Company. The dimension of bagasse particles were 8 to 13 mm length and 0.5 to 2 mm thickness. Its density was 0.12 g/cm^3. Bagasse drying experiments were conducted with an initial moisture content of 180% (based on the dry weight) to study the drying rate of bagasse particles under a moisture content higher than the FSP. Therefore, bagasse particles were mixed with water (with the equivalent weight ratio) for 24 h. The samples were kept in sealed polyethylene bags at 3 to 5 °C for 7 days so that the moisture was distributed evenly. During this period, samples were mixed daily to maintain homogenous moisture content in all bagasse particles.

Drying Process

The drying process of bagasse particles was conducted using a halogen moisture analyzer (Model MB45, OHAUS Company, University of Tehran, Iran) at three temperatures of 105, 120, and 135 °C. The MB45 has a sample capacity of 45 g, with a readability of 0.001 g and repeatability to 0.015% (using a 10 g sample). It is shown in Fig. 1. The heater is a halogen lamp, and the operating temperature range is 50 to 200 ºC in 1º increments. During the drying operation, the moisture content was constantly calculated based on the gravimetric method, and the weight difference between before and after drying to represent the loss of moisture. This drying method is called loss-on-drying (LOD), which is a standard method for measuring moisture. The sample is weighed, receives heat, is dried, and then is weighed again. This device is used for testing moisture and analyzing the moisture content in samples such as wood, pulp, biomass, granules, edible materials, food products, and pastes. A series of tasks were followed to study the drying kinetics of bagasse particles. First, 4 g of bagasse particles was evenly distributed on the surface of a stainless-steel tray for keeping samples inside a halogen dryer chamber. The surface of the tray was covered with an identical thickness of bagasse particles. A decrease in the samples' moisture content at 105, 120, and 130 °C was recorded every 30 seconds to study the effect of temperature on the drying rate of bagasse particles. All experiments were repeated in triplicate for each temperature, and the average values of the moisture content for each temperature were used for drawing and fitting drying curves.

Fig. 1. Halogen moisture Analyzer, MB45 AM (ohaus.com)

Drying Kinetics

Drying is one of the widely used methods for the preservation of cereals, fruits, and vegetables. These models are used for estimating the time in which several products are dried under various drying conditions, improving the efficiency of the drying process, and generalizing drying curves for the design and function of dryers. Equation 1 is used for determining the moisture ratio (MR) of bagasse particles,

$$MR = \left(\frac{M_t - M_e}{M_0 - M_e}\right) \tag{1}$$

where MR is the moisture ratio (dimensionless), M_t is the momentary moisture content per kg of solid matter/kg of water, M_e is equilibrium moisture (kg of material/kg of water), and M_0 is the initial moisture content (kg of material/kg of water), where their values are expressed on a dry basis. In the IR process, samples may be dried as much as dry solid content (Celma *et al*. 2008). Especially for long drying times, M_e is relatively small in

comparison with M_t or M_0. Therefore, Therefore, Eq. 1 is simplified as Eq. 2 (Shah and Josh 2010; Doymaz *et al*. 2007).

$$MR = \left(\frac{M_{t+dt}}{M_0}\right) \tag{2}$$

The evaporation ratio in bagasse particles was calculated using Eq. 3,

$$DR = \left(\frac{M_{t+dt}-M_t}{dt}\right) \tag{3}$$

where DR is the drying rate (kg/s), M_{t+dt} is the moisture content (kg water/kg d.b) at the time $t + dt$, M_t is the moisture content in the time t, and t is the drying time (s). To determine the MR in this study, experimental data were examined for 18 most important and commonly used models that are used to predict the MR of food and other agricultural products (Table 1). The fixed variables and the constant drying of each TLD model were analyzed and obtained based on the time (the independent variable) using MATLAB 2016 software. The best model was determined using three statistical parameters, namely coefficient of determination (R^2), root mean square error (RMSE), and the sum of squared errors (SSE). The fit of a model with the highest value for R^2 and lowest values for SSE and RMSE best describes the drying characteristics of bagasse particles. The values for R^2, RMSE, and SSE were calculated using Eqs. 4, 5, and 6, respectively,

$$R^2 = \frac{\sum_{i=1}^{N}(MR_{\exp,i} - \overline{MR}_{\exp})(MR_{pre,i} - \overline{MR}_{pre})}{\sqrt{\left[\sum_{i=1}^{N}(MR_{\exp,i} - \overline{MR}_{\exp})^2\right]\left[\sum(MR_{pre,i} - \overline{MR}_{pre})^2\right]}} \tag{4}$$

$$RMSE = \left[\frac{1}{N}\sum_{I=1}^{n}(M_{pre,i} - M_{\exp,i})\right]^{1/2} \tag{5}$$

$$SSE = \sum_{i=1}^{n}(MR_{pre,i} - MR_{\exp})^2 \tag{6}$$

where $M_{\exp i}$ and $M_{pre,i}$ are respectively the observed and model-predicted bagasse particles moisture contents in the ith measurement, , N is the number of observations (data), and n is the number of constants used in the equation.

Artificial Neural Network Model

The multilayer perceptron (MLP) is a widely used and practical ANN model that was chosen from the ANN toolbox of MATLAB v.16 to predict the MR. In this model, the drying time and temperature of bagasse particles and MR were introduced as the input and output data, respectively. To acquire a suitable topology of the ANN, it is trained with experimental data, and the best topology was determined by trial and error and minimizing the ANN error (Sadeghi *et al*. 2019; Haftkhani *et al*. 2021).

The mathematical equation of the MLP ANN is as follows,

$$Y = g\left(\theta + \sum_{j=1}^{m} v_j \left[\sum_{i=1}^{n} f(W_{ij}X_i + \beta_j)\right]\right) \tag{7}$$

where Y is the dependent variable, g (.) is the activation function of output neurons, θ is the bias value for output neurons, v_j is the value of weights between the jth output neuron and hidden neurons, f (.) is the activation function of hidden neurons, W_{ij} is the weights between

the jth input neuron and the jth hidden neuron, X_i is the input value of the ith dependent variable, and β_j is the jth hidden neuron bias.

Table 1. Mathematical Models Applied to Drying Curves

Model name	Model equation	Reference
Lewis (Newton)	MR = exp(−kt)	Ghazanfari *et al.* (2006)
Henderson and Pabis	MR = a exp(−kt)	Kaur and Singh (2014)
Logarithmic	MR = a exp(−kt) + b	Gan and Poh (2014)
Modified Midilli *et al.*-III	MR = a exp(−kt) + bt	Kaur and Singh (2014)
Two-term	MR = a exp(−k_1 t) + b exp(−k_2 t)	Kumar *et al.* (2014)
Noomhorm and Verma	MR = a exp(−k_1 t) + b exp(−k_2 t) + c	Kaleta and Gornicki (2010)
Modified Henderson and Pabis	MR = a exp (−k_1 t) + b exp(−k_2 t) + c exp(−k_3 t)	Erbay and Icier (2009)
Two-term exponentia	MR = a exp(−kt) + (1 − a) exp(−akt)	Lee and Kim (2009)
Modified two term-V	MR = a exp(−kt) + (1 − a) exp(−gt)	Verma *et al.* (1985)
Page	MR = exp (−kt^n)	Doymaz (2007a)
Modified Page-IV	MR = a exp(−kt^n)	Babalis *et al.* (2006)
Hii *et al*	MR = a exp (−kt^n) + b exp(−gt^n)	Hii *et al.* (2009)
Kaleta *et al*. II	MR = a exp(−kt^n) + (1 − a)exp(−gt^n)	Kaleta *et al.* (2013)
Modified Page II	MR = exp[−$(kt)^n$]	Vega *et al.* (2007)
Modified page .III	MR = a exp[−$(kt)^n$]	Ertekin and Firat (2017)
Demir *et al.*	MR = a exp[−$(kt)^n$] + b	Demir *et al.* (2007)
Wang and Singh	MR = 1 + at + bt^2	Wang and Singh (1978)
Midilli *et al.*	MR = a exp(−kt^n) + bt	Midilli *et al.* (2002)

In this study, 70, 15, and 15% of the data were randomly selected for training, validation, and testing purposes, respectively. The Levenberg-Marquardt algorithm was chosen for training data. The activation function of the output neuron was linear, but that of the hidden neuron was a hyperbolic-tangent-sigmoid function as follows,

$$f(x) = \frac{2}{1+e^{(-2x)}} - 1 \qquad (8)$$

where $f(x)$ and x are neurons' output and input values, respectively. The structure of MLP for predicting MR is shown in Fig. 2. Also, it was reported in earlier works (Sadeghi *et al.* 2019; Haftkhani *et al.* 2021) that a network with one hidden layer and hyperbolic tangent sigmoid (tansig) function is commonly used for forecasting in practice. The statistical parameters MSE, MAPE, and R^2 were used for assessing the efficiency of the ANN model to investigate the error value and match the real and predicted data. These statistical parameters were calculated using Eqs. 9, 10, and 11,

$$MAPE = \frac{1}{n}\sum_{i=1}^{n}\left(\frac{|y_{exp.}-y_{pred.}|}{y_{exp.}}\right)100 \qquad (9)$$

$$MSE = \frac{1}{n}\sum_{i=1}^{n}\left(y_{exp.} - y_{pred.}\right)^2 \qquad (10)$$

$$R^2 = 1 - \frac{\sum_{i=1}^{n}(y_{exp.} - y_{pred.})^2}{\sum_{i=1}^{n}(y_{exp.} - \overline{y_{exp.}})^2} \qquad (11)$$

where y_{exp} and y_{pred} are the real and predicted data, respectively, $\overline{y_{exp.}}$ is the average of real data, and n is the number of data.
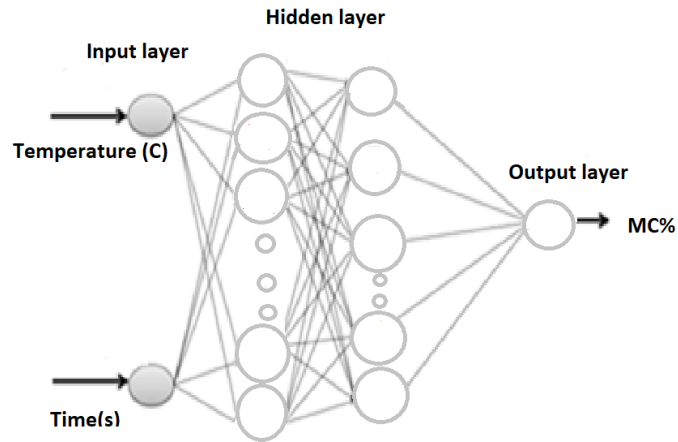
Fig. 2. Schema of artificial neural network for prediction moisture content of bagasse particle

RESULTS AND DISCUSSION

To change the anatomy and position of moisture in hygroscopic materials, the temperature is used both directly and indirectly during the drying process. Changes in the bagasse MR in different temperatures over time, influenced by the direct heat transfer, on the surface of bagasse particles are shown in Fig. 3, indicating an exponential reduction in the bagasse MR during the drying process. The bagasse particle MR at 105, 120, and 135 °C approached zero in 1110, 630, and 420 seconds, respectively. The change in the moisture content of bagasse particles was significantly influenced by increasing the temperature from 105 to 135 °C (an increase of 30 °C), which reduced the bagasse drying time (reducing the bagasse moist content) by 2.7 times (Fig. 3).
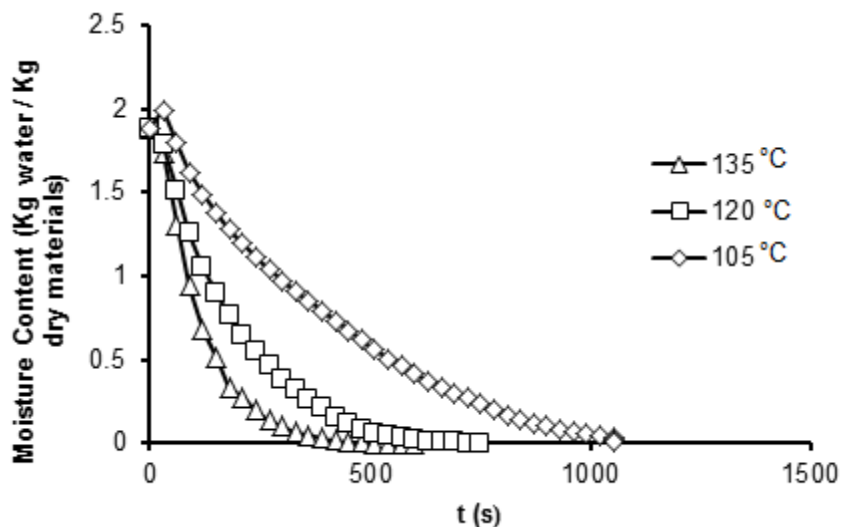
Fig. 3. Moisture content versus drying time at different halogen drying temperature

Drying with halogen radiation involves heating with electromagnetic radiation having a wavelength ranging from 0.76 to 2.5 μm. Halogen radiant energy can be easily passed through the air without heating the ambient air. When the halogen lamp is radiated toward the cellulosic materials, in general, reflection varies within the range between 10 and 30%, and the penetration depth of the radiation is close to 0.3 mm. This means that the cellulosic materials surface absorbs 70 to 90% of all incident IR radiation. So, the surface of cellulosic materials becomes strongly heated and then a thermal gradient within the material significantly increases in a short period by conduction. In most previous studies, the impact of temperature on the bagasse drying process was studied indirectly using hot-air dryers. Recently, the direct radiation of IR and microwave dryer has been used in a few studies, indicating a reduction in the drying period using infrared radiation compared with the hot air dryers, especially in the falling drying rate period (Huang *et al*. 2021). Infrared energy penetrates into the materials and then is converted to heat without heating the adjacent air. Thus, the internal part of materials would be warmer than the surrounding air and the rate of heat transfer is greater as compared to the hot air drying technique (Huang *et al*. 2021; Al-Hilphy *et al*. 2021). Figure 4 shows the bagasse drying rate against its moisture content. Accordingly, the slope of drying curves changes during the drying period of bagasse particles. Depending on the physical features and the moisture content of the materials, the drying process of hygroscopic materials takes place in three separate stages, including the constant drying rate and the first and the second falling rate period of drying. According to Fig. 5, a constant drying rate was not observed in any of the drying temperatures of bagasse particles, and the whole drying process of bagasse particles happened during the falling rate period of drying. Vijayaraj *et al*. (2007) dried bagasse particles in at 80 to 120 °C and an air velocity of 0.5 to 2 m/sec. Their results showed that the entire drying process happened in the falling rate period of drying despite a high initial moisture content of bagasse. Freire *et al*. (2001) and Shah and Joshi (2010) observed no constant drying rate in the drying process of bagasse. Du *et al*. (2005) investigated the drying process of wood chips in convective and microwave dryer. Their results showed that the value for the output moisture microwave dryer was approximately twice that of convective dryers in the initial 100 seconds.
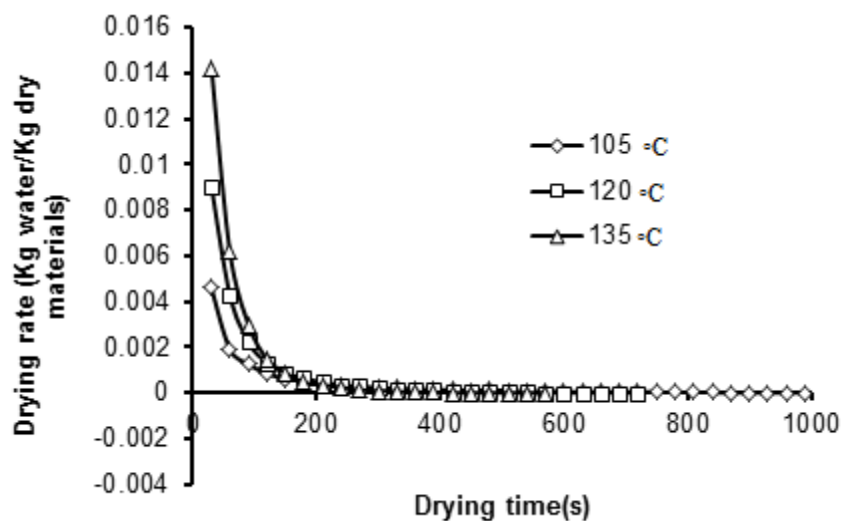
Fig. 4. Drying rate versus drying time at different halogen drying temperature

When the moisture of the surface layer in the sample evaporates very quickly, the surface of particles dries very quickly with shrinkage, which reduces the diameter of cellular pores and cavities. Therefore, quick transfer and moisture extraction from the lower layers close to the surface of particles are not possible when there is free water in the lower layers of the surface layer. In fact, the moisture evaporation rate from the surface of the particles is faster than the surface layer's rate of feeding moisture from its lower layers. Therefore, it is not possible to observe a constant drying rate. In this study, using the halogen lamp and direct transfer of the temperature to bagasse particles caused a fast reduction of the water-air interface and its fast recess to the pores near the surface. As a result, it was difficult to observe a constant drying rate. This type of drying behavior can also be interpreted based on the Biot (Bi) number. For solid materials with a Bi number less than 0.1, the process of drying takes place at a constant rate (Sander *et al*. 2001), while the Bi number for lignocellulosic materials has been reported to be more than 0.2 (Soni 2007). The first (A-B) and second (B-C) falling rate periods of drying are obvious in the curves of the bagasse drying rate, (Fig. 5). In the first falling rate period of drying, the moisture moves from lower layers from the wood surface to its outer surface (from higher to lower concentrations), which is influenced by the diffusion mechanism. At the beginning of this period, wood surface lower layers are rich in moisture and the drying rate of bagasse particles is high, with a steeper slope of particle drying curves. The moisture content of particles' lower layers is reduced over time, making the moisture exhaust from bagasse particles more difficult. This increases the surface temperature of the particles, and a temperature gradient is formed contrary to the direction of the moisture gradient in the particles. In lower moisture contents, a sharp deviation is observed in the slope of the drying curve, suggesting that there is no free water available in this stage of drying, with a completely dry surface of fibers. Therefore, this minimizes the drying rate of particles and increases the drying period. This period of drying is known as the second falling rate period of drying.
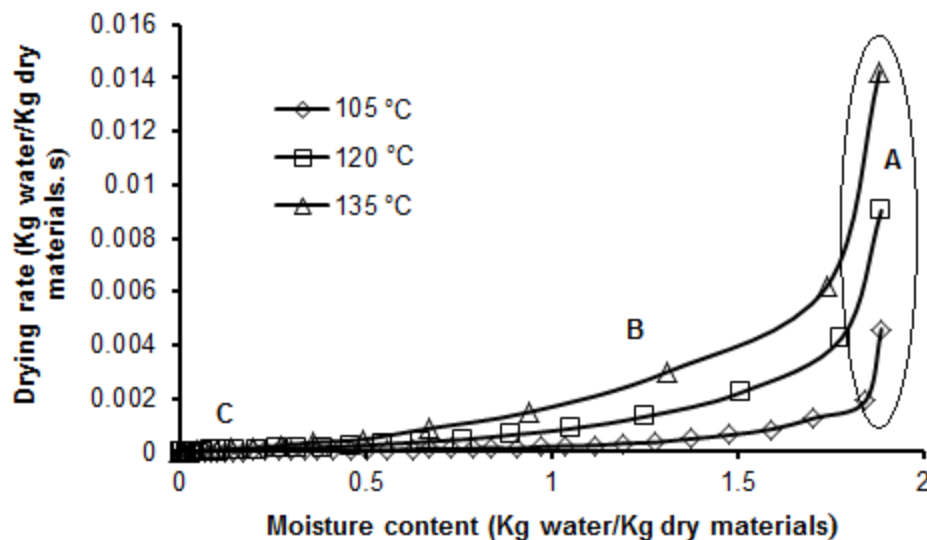
Fig. 5. Drying rate versus moisture content at different halogen drying temperature

Drying Curves Fitting

Modeling the drying process of agricultural products is based on a collection of accurate and simple mathematical equations that can adequately describe various conditions of the drying process and drying materials. Eighteen models (Table 1) were fitted on the drying curves obtained from the experimental data using MATLAB 2016 software. The best TLD model was selected based on a higher value of R^2 and lower values of SSE and RMSE. The results from the fit of mathematical models on the experimental data showed that the Hii *et al*. model had the best fit on the experimental data. The Hii *et al*. model is a combination of the Page and two-term drying model (Hii *et al*. 2009).

The results from the fit of mathematical models on the experimental data with their fixed coefficients and the values for statistical parameters at different temperatures are shown in Tables 2, 3, and 4. A careful inspection of these results revealed that there was only a limited difference between the results of Hii *et al*. model as best model and other TLD models. According to Tables 2, 3, and 4, most of TLD models showed relatively high values of R^2 (0.9995) and lower values of SSE and RMSE (0.001213 and 0.007601). Some of the models given in Tables 2 to 4 are derived from the based model and were modified by increasing the number of parameters.

Since, the effect of different parameter values on the drying curve shape is always not significant, some drying model showed the same fit with each other. Thus there was no reason to use complex models for drying data. For example, results showed that Henderson and Pabis model with 2 parameters and Logarithmic, Modified Midilli *et al*.-III, Modified page II and Modified Page-IV models with 3 parameters showed good fitness and prediction of moisture content of bagasse particles (R^2>0.99), and there was no significant different among these models and the Hii *et al* model based statistical index (R^2, RMSE AND SSE). Therefore, it should be noted that a simple model with the same degree of fit or with a slight loss of goodness of-fit can be used instead of a complex model. Buzrul (2022), proposed that complex models or models that have more than three parameters and models that have the same fit with another model but have more adjustable parameters can be safely eliminated without hesitation. Hence, among the 18 selected models, statistical analysis implied that the Modified Henderson and Pebis model with only two parameters could accurately predict changes in moisture content of bagasse particle.

Artificial Neural Network Model

Experimental data were categorized into three classes for modeling with the ANN. Accordingly, 70, 15, and 15% of the data were considered for training, validation, and testing of the ANN model, respectively. The ANN model with topologies of 2-5-1 and 2-20-1, with one hidden layer presented the best results for prediction of variations in moisture content of bagasse particles. If the computing time and simplicity of the topology are considered, the best choice is the topology of 2-5-1. Based on the results in Table 5, the mean absolute percent error (MAPE) and R for the whole dataset in the ANN for predicting MR is 2.61% and 0.99969, respectively. A high R^2 and a low error (%) between experimental and predicted data shows that the ANN can better predict the bagasse MR than Hii *et al*. model.

bioresources.com

Table 2. Statistical Results and Drying Constant of Mathematical Models at Different Temperature Drying (T=105 °C)

T°C	Model Equation	R^2	Constants	RMSE	SSE
105 °C	$f(x) = \exp(-kt)$	0.9850	k = 0.006706	0.07281	0.1007
	$f(x) = a\exp(-kt)$	0.9909	a = 1.949, k =-0.002802	0.05269	0.1083
	$F(x)=a\exp(-kt)+b$	0.9983	a = 2.047, k = 0.002217, b = -0.1695	0.02282	0.0198
	$F(x)=a\exp(-kt) + bt$	0.9978	a = 1.883, k = 0.002379, b = -0.0001286	0.02532	0.07116
	$F(x)=a\exp(-k_1 t)+c\exp(-k_2 t)$	0.9914	a =-0.08839, k_1 =0.9134, k_2 =0.002837, c = 1.974	0.05268	0.1027
	$F(x)=a\exp(-k_1 t) + c\exp(-k_2 t) +d$	0.99917	a =2.003, k_1 =0.002038, k_2 = 0.9134, d = -0.2112	0.04202	0.01053
	$F(x)=a\exp(-k_1 t) + c\exp(-k_2 t) + d\exp(-k_3 t) +d$	0.9914	a =1.974, k_1 = 0.002837, k_2 = 0.975, k_3 =0.5469, c = -0.1334, d = 0.04506	0.05416	0.1027
	$F(x)=a\exp(-k_1 t) +(1-a)\exp(-ak_2 t)$	0.9259	a =1.974, k_1 = 0.002837, k_2 =0.9134	0.1527	0.8863
	$F(x)=a\exp(-kt) +(1-a)\exp(-gt)$	0.9253	a =1.974, k =0.002837, g=0.975	0.1527	0.8863
	$F(x)=a\exp(-kt^n)$	0.9941	a =1.837, b = 0.0009851, n = 1.161	0.04295	0.07009
	$F(x)=\exp(-kt^n)$	0.83	k =5e+05, n =0.9706	0.2232	1.944
	$F(x)=a\exp(-kt^n) + (1-a)\exp(-gt^n)$	0.9291	a =1.785, k =0.0007033, g =2.978, n = 1.211	0.1515	0.8489
	$F(x)=a\exp(-kt^n) + c\exp(-gt^n)$	0.9995	a =1.294, k =1.367e-05, c = 0.5862. g =0.0002719, n = 1.786	0.01333	0.006401
	$F(x)=a\exp(-kt^n)+bt$	0.8484	a =1.242, k =0.01256, b =-0.001228, n = -9.701	0.2214	1.814
	$F(x)=1+at+bt^2$	0.7426	a = -0.0007124, b= -2.295e-07	0.281	3.08
	$F(x)=a\exp[-(kt)^n]$	0.994	a =1.83, b = 0.002531, n = 1.166	0.0435	0.07189
	$F(x)= \exp[-(kt)^n]$	0.9822	b =0.001611, n = 2.395	0.07392	0.2131
	$F(x)=a\exp[-(kt)^n]+b$	0.9938	a =1.827, b = 0.002536 , n = 1.166	o.04414	0.07402

bioresources.com

Table 3. Statistical Results and Drying Constant of Mathematical Models at Different Temperature Drying (T=120 °C)

T°C	Model Equation	R^2	Constants	RMSE	SSE
120 °C	$f(x) = \exp(-kt)$	0.9881	$k = 0.003745$	0.06306	0.09942
	$f(x) = a \exp(-kt)$	0.999	$a = 2.116$, $b = 0.00577$	0.01889	0.008567
	$F(x)=a \exp(-kt) +c$	0.9983		0.02282	0.0198
	$F(x)=a \exp(-kt) +c \exp(-k_2t)$	0.9975	$a =2.157$, $b = 0.005964$, $k =0.9134$, $c = -0.2919$	0.03085	0.02094
	$F(x)=a \exp(-kt) + c \exp(-k_1t) +d$	0.9995	$a =2.155$, $k =0.005375$, $k_1 =0.9134$, $c =-0.2292$, $d =-0.06012$	0.02445	0.004384
	$F(x)=a \exp(-k_1t)+c \exp(-k_2t)+d \exp(-k_3t)$	0.9975	$a =2.158$, $k_1 =0.005965$, $b_2 = 0.9134$, $b_3 =0.2735$, $c =-0.402$, $d = 0.1097$	0.03236	0.02094
	$F(x)=a \exp(-kt) +(1-a) \exp(-ak_1t)$	0.9763	$a =2.134$, $k =0.00585$, $k_1 = 0.9134$	0.09278	0.198
	$F(x)=a \exp(-kt) + (1-a) \exp(-gt)$	0.9763	$a =2.134$, $k =0.00585$, $g =0.9134$	0.09278	0.198
	$F(x)=a \exp(-kt^n)$	0.9981	$a = 1.898$, $k =0.001704$, $n = 1.208$	0.02652	0.01617
	$F(x)=\exp(-kt^n)$	0.6957	$k =1.629e-08$, $n =2.979$	0.3207	6.581
	$F(x)=a \exp(-kt^n) + (1-a) \exp(-gt^n)$	0.9653	$a =1.954$, $k =0.002078$, $g = 1.403$, $n =1.178$	0.1148	0.29
	$F(x)=a \exp(-k t^n) + c \exp(-g t^n)$	0.9995	$a =1.125$, $k=2.499e-05$, $c = 0.7501$, $g = 0.00024$, $n = 1.87$	0.007601	0.001213
	$F(x)=a \exp(-kt^n) + bt$	0.9984	$a =1.907$, $k = 0.002072$, $c = -3.828e-05$, $n = 1.168$	0.02442	0.01311
	$F(x)=1+at+bt^2$	0.7265	$a = -0.002029$, $k =7.124e-07$	0.3084	2.282
	$F(x)=a \exp[-(kt)^n]$	0.9981	$a =1.898$, $k = 0.0051$, $n = 1.208$	o.02652	0.01617
	$F(x)= \exp[-(kt)^n]$	0.972	$k = 0.003214$, $n =2.116$	0.9868	0.2337
	$F(x)=a \exp[-(kt)^n] + b$	0.9984	$a =1.937$, $b = 0.00498$, $c =-0.02897$, $n = 1.16$	0.02445	0.01316

bioresources.com

Table 4. Statistical Results and Drying Constant of Mathematical Models at Different Temperature Drying (T=135 °C)

T°C	Model	R^2	Constants	RMSE	SSE
135 °C	$f(x) = \exp(-kt)$	0.9855	k =0.006706	0.07281	0.1007
	$f(x) = a\exp(-kt)$	0.9977	a =2.366, b = 0.01029	0.02914	0.01528
	$F(x)=a\exp(-kt)+c$	0.9886	a =2.083, b =0.008413, c = -0.05057	0.06703	0.07638
	$F(x)=a\exp(-k_1t) + c\exp(-k_2t)$	0.9994	a =2.411, k = 0.01053, k_1 =0.975, c =-0.5302	0.01536	0.003775
	$F(x)=a\exp(-k_1t) +c\exp(-k_2t) +d$	0.9995	a =2.402, k =0.01029, k_1 =0.975, c =-0.5089, d =-0.01262	0.001748	0.002727
	$F(x)=a\exp(-k_1t) +c\exp(-k_2t) +d\exp(-k_3t)$	0.9994	a = 2.411, k_1 =0.01054, k_2 =0.975, k_3 = 0.5469, c =-0.2046, d = -0.3261	0.01642	0.003775
	$F(x)=a\exp(-k_1t) +(1-a)\exp(-ak_2t)$	0.8842	a = 2.411, k_1 =0.01054, k_2 = 0.975	0.2141	0.7795
	$F(x)=a\exp(-kt) +(1-a)\exp(-gt)$	0.8840	a =2.411, k =0.01054, g =0.9649	0.2141	0.7795
	$F(x)=a\exp(-kt^n)$	0.997	a =1.932, k =0.001844, n = 1.312	0.03431	0.02001
	$F(x)=\exp(-kt^n)$	0.7774	k =6.524e-07, n =2.718	0.2882	1.495
	$F(x)=a\exp(-kt^n) +(1-a)\exp(-gt^n)$	0.8841	a =2.288, k =0.007153, g =0.9649, n =1.07	0.2206	0.7784
	$F(x)=a\exp(-kt^n)+ c\exp(-gt^n)$	0.9995	a = 2.288, k = 0.007151, g = 0.975, c =-0.4077, n =1.07	0.001326	0.001638
	$F(x)=a\exp(-kt^n) + bt$	0.9769	a=0.02299, b=-0.001318, k=-5.648, n=-0.06798	0.09136	0.1753
	$F(x)=1+at+bt^2$	0.9531	a = -0.004318, b =4.627e-06	0.1323	0.3149
	$F(x)=a\exp[-(kt)^n]$	0.997	a =1.932, k =0.008252, n =1.312	0.03431	0.02001
	$F(x)= \exp[-(kt)^n]$	0.7775	k =0.005315, n =2.791	0.2882	1.495
	$F(x)=a\exp[-(kt)^n] + b$	0.9972	a =1.913, k = 0.008354, c =0.01465, n =1.344	0.03409	0.0186

Table 5. Evaluation the Performance of Neural Network using Statistical Parameters

Factor	Parameter	R	MSE	MAPE
MR	training	0.99985	0.00006	
	validation	0.99944	0.000049	
	testing	0.99915	0.000243	
	All data	0.99969		2.61

Figure 6 shows R values for MR for training (0.99985), validation (0.99944), and testing (0.99915) data in the ANN model. The ANN uses the ability of machine learning algorithms, based on which the ANN can improve its functionality based on previous training and experiences.
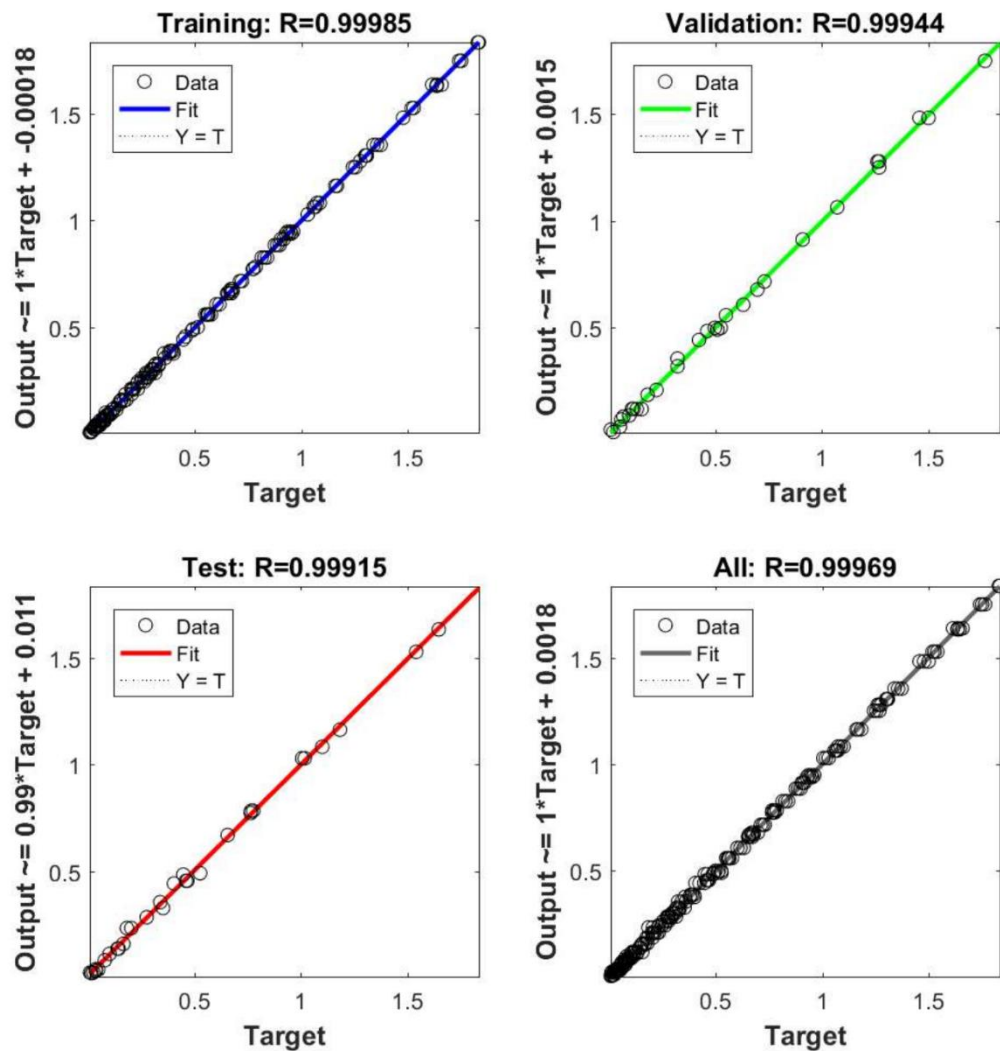
Fig. 6. Regression plots of the developed ANN model for (a) the training data set, (b) the validation data set, (c) the testing data set, and (d) All data

If the training is correct, the designed and selected algorithm can estimate the correct answer for new observations. In the case of changing data, the produced program can also adapt itself to new conditions. The ANN is distinguished from other modeling methods and yields better results than other modeling methods due to its better generalizability and adaptability. The fit of real data against predicted data with the ANN suggests that the values of MR predicted by the ANN model better match the real data (Fig. 7). The drying process of solid materials and other lignocellulosic materials was predicted using the ANN in many studies, all of which used statistical parameters, such as MAPE, MSE, and R^2, as the main indexes for comparing experimental and predicted data.
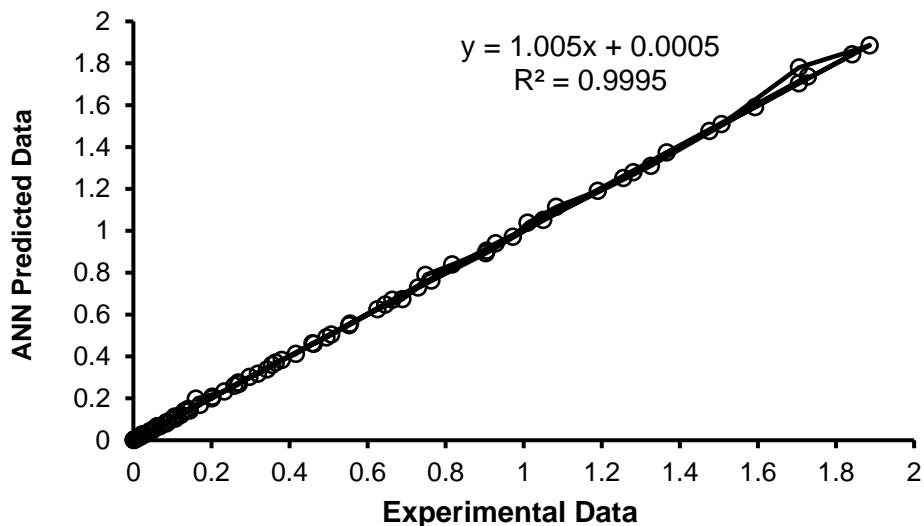
Fig. 7. Comparison of measured and predicted data with ANN model

The results from these studies correspond to those of other research (Celma *et al*. 2008; Sadeghi *et al*. 2019; Saxena *et al*. 2022). The main obstacle in training ANNs is overfitting. This obstacle occurs when the ANN functions properly on training data and no other data series. Figure 8 shows the efficiency of prediction for the ANN based on epochs. The calculation is stopped in the ANN when the error resulting from validation data remains unchanged for six consecutive epochs. As shown in Fig. 8, predicting MR has continued for 11 epochs, but predicting and processing data have stopped as the error has remained unchanged for six consecutive epochs (after the latter 11 epochs). Thus, the network was trained, validated, and tested appropriately so that an adequate convergence exists between the prediction ability of training, validation, and testing data based on MSE in the 11th epoch for predicting MR. Before proposing the ANN models as best model for the drying of bagasse particles, it is important to note that findings in current work demonstrated that selected ANN model and a number of semi-empirical models such as Midilli *et al*., Logarithmic, Henderson and Pabis, Modified Midilli *et al*.-III, Modified page II and Modified Page-IV models could precisely predicted the moisture of bagasse particle with determination coefficient higher than 0.999. Therefore, the models with the less than 3 parameters provided good agreement and can be considered a promising tool to predict drying kinetic of bagasse particles. Sadeghi *et al* (2019) listed 100 models, including feed-forward neural networks that could be used for thin-layer modeling and reported that the most of the drying curves can be described by models with only two adjustable parameters.
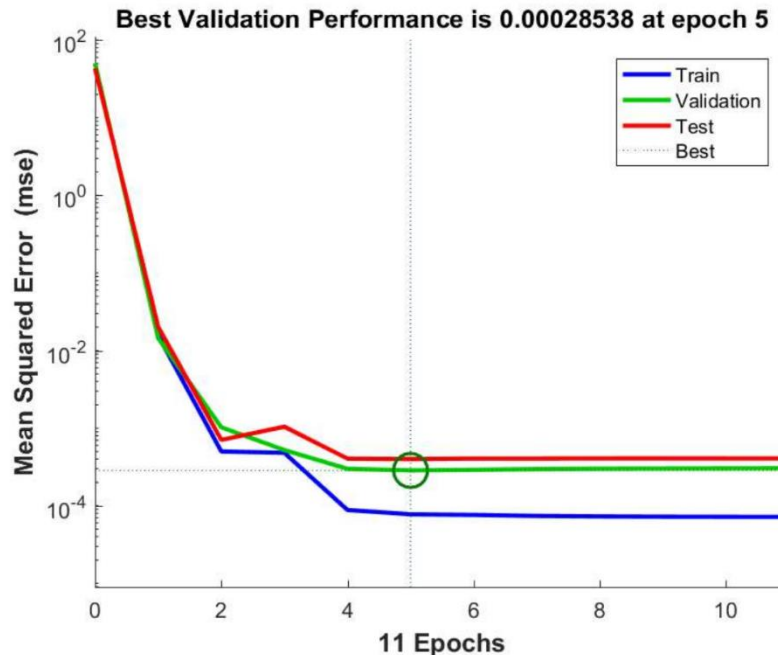
Fig. 8. Neural network performance by period (epoch) for training, validation, and testing data

CONCLUSIONS

1. This study showed that an increase in the temperature elevated the drying rate, thereby reducing the total time of drying. The drying curves of bagasse particles also showed that the whole drying period occurred with a falling rate, and no constant drying rate was observed in bagasse particles.

2. The Hii *et al*. model better matched the experimental data than the other thin drying layer models according to three statistical parameters of R^2, SSE, and RMSE.

3. The ANN yielded more adequate results than all the other mathematical models. A careful inspection of the results of this study revealed that the selected ANN topology and a number of thin drying layer models could precisely predicted the drying process of bagasse particle with determination coefficient higher than 0.99. Therefore, it should be emphasized that it not necessary to use and test all the models have been applied for describe the drying kinetics of bagasse particles.

4. A simple model like the Henderson & Pabis model with two parameters (*a* and *k*) and acceptable accuracy can be more useful than complex models or models that have more than two parameters for modeling lignocellulosic materials.

ACKNOWLEDGEMENTS

Competing Interests

The authors have no relevant financial or non-financial interests to disclose.

Author Contributions

All authors contributed to the study conception and design. Material preparation, data collection and analysis were performed by Mohammad Arabi and Mohammad Dahmardeh Ghalehno. The first draft of the manuscript was written by Mohammad Arabi and all authors commented on previous versions of the manuscript. All authors read and approved the final manuscript.

Author Statements

The authors certify that they have participated sufficiently in the work to take public responsibility for the content. Furthermore, each author certifies that this material or similar material has not been and will not be submitted to or published in any other publication before its appearance in *BioResources*.

Data Availability Statements

The datasets generated during and/or analysed during the current study are available from the corresponding author on reasonable request.

REFERENCES CITED

Adejumo, I. O., and Adebiyi, O. A. (2020). "Agricultural solid wastes: Causes, effects, and effective management," *Strategies of Sustainable Solid Waste Management* 15*, 8.* DOI: 10.5772/intechopen.93601

Al-Hilphy, A. R., Gavahian, M., Barba, F. J., Lorenzo, J. M., Al-Shalah, Z. M., and Verma, D. K. (2021). "Drying of sliced tomato (*Lycopersicon esculentum* L.) by a novel halogen dryer: Effects of drying temperature on physical properties, drying kinetics, and energy consumption," *Journal of Food Process Engineering* 44(3), article e13624. DOI: 10.1111/jfpe.13624

Arabi, M., Faezipour, M., Layeghi, M., Khanali, M., and Hosseinabadi, Z. (2017). "Evaluation of thin-layer models for describing drying kinetics of poplar wood particles in a fluidized bed dryer," *Particulate Science and Technology* 35(6), 723-730. DOI: 10.1080/02726351.2016.1196275

ASTM Standard D6980-12 (2012). "Standard test method for determination of moisture in plastics by loss in weight," ASTM International, West Conshohocken, PA, USA.

Babalis, S. J., Papanicolaou, E., Kyriakis, N., and Belessiotis, V. G. (2006). "Evaluation of thin-layer drying models for describing drying kinetics of figs (*Ficus carica*)," *Journal of Food Engineering* 75(2), 205-14. DOI: 10.1016/j.jfoodeng.2005.04.008.

Bahadori, A., Zahedi, G., Zendehboudi, S., and Jamili, A. (2012). "Estimation of the effect of biomass moisture content on the direct combustion of sugarcane bagasse in boilers," *International Journal of Sustainable Energy* 33(2), 349-356. DOI: 10.1080/14786451.2012.748766

Boopathy, R., Asrabadi, B.R., and Ferguson, T.G. (2002). "Sugar cane (*Saccharum officinarum* L) burning and asthma in Southeast Louisiana, USA," *Bulletin of Environmental Contamination and Toxicology*. 68(2), 173-9. DOI: 10.1007/s001280235

bioresources.com

Brys, A., Kaleta, A., Górnicki, K., Głowacki, S., Tulej, W., Bry´, J., and Wichowski, P. (2021). "Some aspects of the modelling of thin-layer drying of sawdust," *Energies* 14, article 726. DOI: 10.3390/en14030726.

Buzrul, S. (2022). "Reassessment of thin-layer drying models for foods: A critical short communication," *Processes* 10(1), article 118. DOI: 10.3390/pr10010118

Celma, A. R., Rojas, S., and Lopez-Rodriguez, F. (2008). "Mathematical modelling of thin-layer infrared drying of wet olive husk," *Chemical Engineering and Processing*: *Process Intensification* 47(9-10), 810-1818. DOI: 10.1016/j.cep.2007.10.003

Chai, H., Chen, X., Cai, Y., and Zhao, J. (2019). "Artificial neural network modeling for predicting wood moisture content in high frequency vacuum drying process," *Forests* 10(1), 16. DOI: 10.3390/f10010016

Dash, K. K., Chakraborty, S., and Singh, Y. R. (2020). "Modeling of microwave vacuum drying kinetics of bael (*Aegle marmelos* L.) pulp by using artificial neural network," *Journal of the Institution of Engineers (India):* Series A, pp.1-9. DOI: 10.1007/s40030-020-00431-x.

Demir, V. E., Gunhan, T. U., and Yagcioglu, A. K. (2007). "Mathematical modelling of convection drying of green table olives," *Biosystems Engineering* 98(1), 47-53. DOI: 10.1016/j.biosystemseng.2007.06.011

Doymaz, I. (2007). "Air-drying characteristics of tomatoes," *Journal of Food Engineering* 78, 1291-1297. DOI: 10.1016/j.jfoodeng.2005.12.047

Du, G., Wang, S., and Cai, Z. (2005). "Microwave drying of wood strands," *Drying Technology* 23(12), 2421-2436. DOI: 10.1080/07373930500340494.

EL-Mesery, H. S., and El-khawaga, S. E. (2022). "Drying process on biomass: Evaluation of the drying performance and energy analysis of different dryers," *Case Studies in Thermal Engineering* 1(33), article 101953. DOI: 10.1016/j.csite.2022.101953

Erbay, Z., and Icier, F. (2009). "Optimization of drying of olive leaves in a pilot-scale heat pump dryer," *Drying Technology* 27(3), 416-427. DOI: 10.1016/j.jfoodeng.2008.10.004

Ertekin, C., and Firat, M. Z. (2017). "A comprehensive review of thin-layer drying models used in agricultural products," *Critical Reviews in Food Science and Nutrition* 57(4), 701-717. DOI: 10.1080/10408398.2014.910493.

Freire, F., Figueiredo, A., and Ferrao, P. (2001). "PH—Postharvest technology: Modelling high temperature, thin layer, drying kinetics of olive bagasse," *Journal of Agricultural Engineering Research* 78(4), 397-406. DOI: 10.1006/jaer.2000.0657.

Gan, P. L., and Poh, P. E. (2014). "Investigation on the effect of shapes on the drying kinetics and sensory evaluation study of dried jackfruit," *International Journal of Science and Engineering* 7(2), 193-198. DOI: 10.12777/ijse.7.2.193-198

Ghazanfari, A., Emami, S., Tabil, L. G., and Panigrahi, S. (2006). "Thin-layer drying of flax fiber: II. Modeling drying process using semi-theoretical and empirical models," *Drying Technology* 24(12), 1637-1642. DOI: 10.1080/07373930601031463

Haftkhani, A.R., Abdoli, F., Sepehr, A., and Mohebby, B. (2021). "Regression and ANN models for predicting MOR and MOE of heat-treated fir wood," *Journal of Building Engineering* 42, article 102788.

Han, J., Choi, Y., and Kim, J. (2020). "Development of the process model and optimal drying conditions of biomass power plants," *ACS Omega* 5(6), 2811-2818. DOI: 10.1021/acsomega.9b03557.

Hii, C. L., Law, C. L., and Cloke, M. (2009). "Modeling using a new thin layer drying model and product quality of cocoa," *Journal of Food Engineering* 90(2), 191-198. DOI: 10.1016/j.jfoodeng.2008.06.022

Huang, D., Yang, P., Tang, X., Luo, L., and Sunden, B. (2021). "Application of infrared radiation in the drying of food products," *Trends in Food Science & Technology* 110, 765-777. DOI: 10.1016/j.tifs.2021.02.039

Huang, Y. F., Chiueh, P. T., and Lo, S. L. (2016). "A review on microwave pyrolysis of lignocellulosic biomass," *Sustainable Environment Research* 26(3), 103-109. DOI: 10.1016/j.serj.2016.04.012

Kaleta, A., and Górnicki, K. (2010). "Evaluation of drying models of apple (var. McIntosh) dried in a convective dryer," *International Journal of Food Science & Technology* 45(5), 891-898. DOI: 10.1111/j.1365-2621.2010.02230.x

Kaleta, A., Górnicki, K., Winiczenko, R., and Chojnacka, A. (2013). "Evaluation of drying models of apple (var. Ligol) dried in a fluidized bed dryer," *Energy Conversion and Management* 67, 179-185. DOI: 10.1016/j.enconman.2012.11.011

Kambis, A. D., and Levine, J. S. (1996). "Biomass burning and the production of carbon dioxide: A numerical study," *Biomass Burning and Global Change*. DOI: 10.1016/j2021.111880.

Kaur, K., and Singh, A. K. (2014). "Drying kinetics and quality characteristics of beetroot slices under hot air followed by microwave finish drying," *African Journal of Agricultural Research* 9(12), 1036-1044. DOI: 10.5897/AJAR2013.7759

Kumar, N., Sarkar, B.C., and Sharma, H. K. (2012). "Mathematical modelling of thin layer hot air drying of carrot pomace," *Journal of Food Science and Technology* 49(1), 33-41. DOI: 10.1007/s13197-011-0266-7

Lee, J. H., and Kim, H. J. (2009). "Vacuum drying kinetics of Asian white radish (*Raphanus sativus* L.) slices LWT," *Food Science and Technology* 42(1), 180-186. DOI: 10.1016/j.lwt.2008.05.017

Lemieux, P. M., Lutes, C. C., and Santoianni, D. A. (2004). "Emissions of organic air toxics from open burning: A comprehensive review," *Progress in Energy and Combustion Science* 30(1), 1-32. DOI: 10.1016/j.pecs.2003.08.001

Martinez-Hernandez, E., Amezcua-Allieri, M. A., Sadhukhan, J., and Anell, J. A. (2018). "Sugarcane bagasse valorization strategies for bioethanol and energy production," *Sugarcane-Technology and Research*. DOI: 10.5772/intechopen.72237

Midilli, A. D., Kucuk, H.A., and Yapar, Z. İ. (2002). "A new model for single-layer drying," *Drying Technology* 20(7), 1503-1513. DOI: 10.1081/DRT-120005864

Pang, S. (2000). "Mathematical modelling of MDF fibre drying: Drying optimization," *Drying Technology* 18(7), 1433-1448. DOI: 10.1080/07373930008917786

Raj, L. P., and Stalin, B. (2016). "Optimized design of a bagasse dryer system for sugar industry," *Bonfring International Journal of Industrial Engineering and Management Science*. 1;6(4), 115. DOI: 10.9756/BIJIEMS.7536

Ravindra, K., Singh, T., and Mor, S. (2019). "Emissions of air pollutants from primary crop residue burning in India and their mitigation strategies for cleaner emissions," *Journal of Cleaner Production* 208, 261-273. DOI: 10.1016/j.jclepro.2018.10.031

Ribeiro, de., Souza, J. A., de Farias Neto, S. R., de Lima, E. S., Barbosa de Lima, A. G., and Monteiro Lopes, H. (2019). "Numerical analysis of the sugarcane bagasse drying by cyclone," *Diffusion Foundations* 20, 106-123. DOI: 10.4028/www.scientific.net/DF.20.106

Sadeghi, E., Movagharnejad, K., and Haghighi ASL, A. (2019). "Mathematical modeling of infrared radiation thin-layer drying of pumpkin samples under natural and forced convection," *Journal of Food Processing and Preservation* 43(12), article e14229. DOI: 10.1111/jfpp.14229

Sander, AJ., Kardum, P., and Skansi, D. (2001). "Transport properties in drying of solids," *Chemical and Biochemical Engineering Quarterly* 15(3), 131-138.27.

Saxena, G., Gaur, M. K., and Kushwah, A. (2022). "Performance analysis and ANN modelling of apple drying in ETSC-assisted hybrid active dryer," in: *Artificial Intelligence and Sustainable Computing*, Springer, Singapore, pp. 275-294. DOI: 10.1007/978-981-16-1220-624.

Shah, S., and Joshi, M. (2010). "Modeling microwave drying kinetics of sugarcane bagasse," *International Journal of Electronics Engineering* 2(1), 159-163.

Sharma, G. P., and Prasad, S. (2001). "Drying of garlic (*Allium sativum*) cloves by microwave–hot air combination," *Journal of Food Engineering* 50(2), 99-105. DOI: 10.1016/S0260-8774(00)00200-4

Sicoe, G., Zippenfening, S. E., Simandi, M. D., Szakal, R. A. G. I., and David, I. (2018). "Halogen-drying kinetics of some vegane crackers as fortified food products," *Journal of Agroalimentary Processes and Technologies* 24(4), 311-316.

Soni, S. K. (2007). "A source of energy for 21st century," New India Pub., New Delhi.

Sudhakar, J., and Vijay, P. (2013). "Control of moisture content in bagasse by using bagasse dryer," *International Journal of Engineering Trends and Technology* 4(5), 1331-1333.

Vega, A., Fito, P., Andrés, A., and Lemus, R. (2007). "Mathematical modeling of hot-air drying kinetics of red bell pepper (var. Lamuyo)," *Journal of Food Engineering* 79(4), 1460-1466. DOI: 10.1016/j.jfoodeng.2006.04.028

Verma, L. R., Bucklin, R. A., Endan, J. B., and Wratten, F. T. (1985). "Effects of drying air parameters on rice drying models," *Transactions of the ASAE*. 28(1), 296-0301.

Vijayaraj, B., Saravanan, R., and Renganarayanan, S. (2007). "Studies on thin layer drying of bagasse," *International Journal of Energy Research* 31(4), 422-37. DOI: 10.1002/er.1237.

Wang, C. Y., and Singh, R. P. (1978). "A single layer drying equation for rough rice," *ASAE Paper*. No. 3001; ASAE: St. Joseph, MI, USA.

Zarea Hosseinabadi, H., Doosthoseini, K., and Layeghi, M. (2012). "Drying kinetics of poplar (*Populus deltoides*) wood particles by a convective thin layer dryer," *Drvna Industrija* 63(3), 169-176. DOI: 10.5552/drind.2012.1201

Zhang, T., Huang, J., Deng, S., and Yu, G. (2011). "Influence of pesticides contamination on the emission of PCDD/PCDF to the land from open burning of corn straws," *Environmental Pollution* 159(6), 1744-1748. DOI: 10.1016/j.envpol.2011.01.042